Journal of the European Ceramic Society 22 (2002) 237–245

www.elsevier.com/locate/jeurceramsoc

Creep and stress-rupture behavior of Y_2O_3–Nd_2O_3-doped silicon nitrides with different additive contents

Jian-Wu Cao [a], Akira Okada [a,*], Naoto Hirosaki [b]

[a] *Japan Fine Ceramics Center, Nagoya, 456-8587 Japan*
[b] *National Research Institute for Inorganic Materials, Tsukuba, 305-0044 Japan*

Received 14 December 2000; received in revised form 21 February 2001; accepted 4 March 2001

Abstract

Tensile creep tests were performed on two grades of gas-pressure sintered silicon nitride. Silicon nitride SN4 contained 2.0 mol% Nd_2O_3 and 2.0 mol% Y_2O_3 as sintering aids, and the additives for silicon nitride SN1 were 0.5 mol% Nd_2O_3 and 0.5 mol% Y_2O_3. The delayed failure of SN4 was thought to result from creep rupture because considerable creep deformation was found with a high stress exponent of $n=10.7$ in the stress range of 137 to 220 MPa at 1300°C, and the stress-rupture parameter was determined to be $N=8.4$. The delayed failure of SN1 was thought to result from subcritical crack growth since no significant creep deformation was found and a high stress-rupture parameter of $N=20.7$ was determined. The creep and stress-rupture mechanisms are discussed based on the creep test results and microstructure observation.

Keywords: Creep; Electron microscopy; Sintering aid; Si_3N_4; Stress rupture

1. Introduction

Silicon nitride ceramics are often sintered with oxide additives, which promote densification by forming a liquid phase at elevated temperatures. The liquid phase forms a continuous secondary phase on cooling, either amorphous or partially crystalline. Since the creep behavior of silicon nitride depends on the properties of the secondary phase at high temperatures, the selection of the additives is important for developing creep-resistant ceramics.

Rare earth oxides are widely used as a sintering aid to achieve densification of silicon nitride while maintaining excellent high temperature mechanical properties. It is noteworthy that the selection of the rare earth oxides considerably influences the densification behavior of silicon nitride.[1] and that only 1 mol% addition of rare earth oxides is able to produce dense silicon nitride even by gas pressure sintering without the aid of an applied stress.[2–4] In the case of low additive contents, such as 0.5 mol% Nd_2O_3–0.5 mol% Y_2O_3-doped silicon nitride, densification is achieved through an SiO_2-rich liquid phase, and the oxygen content in the sintered product was reported to be only 0.94 mass %, which is considerably lower than the oxygen content of the original silicon nitride powder.[5] Moreover, silicon nitride with a low sintering aid content exhibits excellent oxidation resistance, in comparison to those with high additive contents, such as 5 mol% Nd_2O_3–5 mol% Y_2O_3.[6]

Tensile creep tests of advanced silicon nitrides have been performed to evaluate the durability at high temperatures.[7–24] This revealed that cavities are extensively generated in tension and that the creep rate is much greater in tension than compression. Also, the cavities generated during tensile creep lead to an extraordinary high stress exponent in Norton's law, in comparison with the compression creep. The stress exponents are in the range of 1 to 2 for compression creep while stress exponents of 3 to 8 are usually obtained in tensile creep tests. The cavitation creep behavior depends on the type of sintering aids used. However, the number of investigations into the effect of composition is limited. Lange et al. performed tensile creep tests of hot-pressed silicon nitrides containing different amounts of MgO, and reported that the creep rate was several times greater in 5% MgO-containing ceramics than 2%.[9] In light of this, silicon nitride with a low additive content, such as 0.5 mol% Nd_2O_3–0.5 mol% Y_2O_3, is expected to exhibit improved creep resistance in comparison to

* Corresponding author.
E-mail address: okada@jfcc.or.jp (A. Okada).

0955-2219/01/$ - see front matter
PII: S0955-2219(01)00250-3

materials with regular additive contents, due to the small amount of grain boundary phase resulting from the very low amount of sintering aids and their low oxygen content. The objective of the present study is thus to investigate the tensile creep behavior of two Nd_2O_3–Y_2O_3-doped silicon nitride ceramics having different amounts of additives.

2. Experimental procedure

Two silicon nitrides, referred hereafter as SN4 and SN1 were investigated in the present study. Both are gas-pressure sintered ceramics but contain different amounts of sintering aids. SN4 was sintered by the addition of 2.0 mol% Nd_2O_3 and 2.0 mol% Y_2O_3, and the additives for SN1 were 0.5 mol% Nd_2O_3 and 0.5 mol% Y_2O_3. The starting powders of Si_3N_4 (beta-type, P21FC, Denka Co. Ltd., Tokyo, Japan), Nd_2O_3 (99.9%, Shin-Etsu Chemical Co. Ltd., Tokyo, Japan) and Y_2O_3 (99.9%, Shin-Etsu Chemical Co. Ltd., Tokyo, Japan) were ball-milled for 94 h in ethanol, subsequently dried in a rotation evaporator and sieved. The powder mixtures were die-pressed at 20 MPa into rectangular bars with dimensions of approximately $100\times30\times5$ mm^3 and then cold isostatically pressed at 200 MPa. The green bodies were sintered at 1950°C for 4 h in a nitrogen atmosphere at a pressure of 1 MPa, followed by sintering in a high-pressure nitrogen gas of 98 MPa at 2000°C for 4 h. The microstructures of the sintered materials are shown in Fig. 1. SN1 exhibits large elongated silicon nitride grains in a matrix of fine silicon nitride grains. The grains are several hundred microns in length with diameters of several microns. SN4 shows a similar texture but the length of the large grains are within several tens of microns and the maximum diameter is approximately ten microns.

Fig. 2 shows a flat dog-bone specimen used for tensile creep testing. The total length of each specimen was 70 mm, with a rectangular cross section of 4.0×2.5 mm^2 in the gauge area. The gauge length was 20 mm.

Creep tests were performed in air using a dead-weight loading apparatus, HTT-300 (Toshin Kogyo Co., Ltd., Tokyo, Japan). The specimens were fixed in hot grips using four silicon carbide pins connected to silicon carbide loading fixtures. The test furnace had six heating elements of $MoSi_2$ and the temperature was controlled to within 5°. The displacements of specimens were measured with an optical image analyzer VAD-1R (Toshin Kogyo Co., Ltd., Tokyo, Japan). Prior to the tests, four strain gauges were glued on to the four planes in the gauge area of the specimen and adjusted to reduce the bending strain of the specimen. The four plane strains, ε_1, ε_2, ε_3, and ε_4, were measured with a strain amplifier and the subscripts 1 and 2 correspond to opposite planes of 3 and 4, respectively. The bending strain

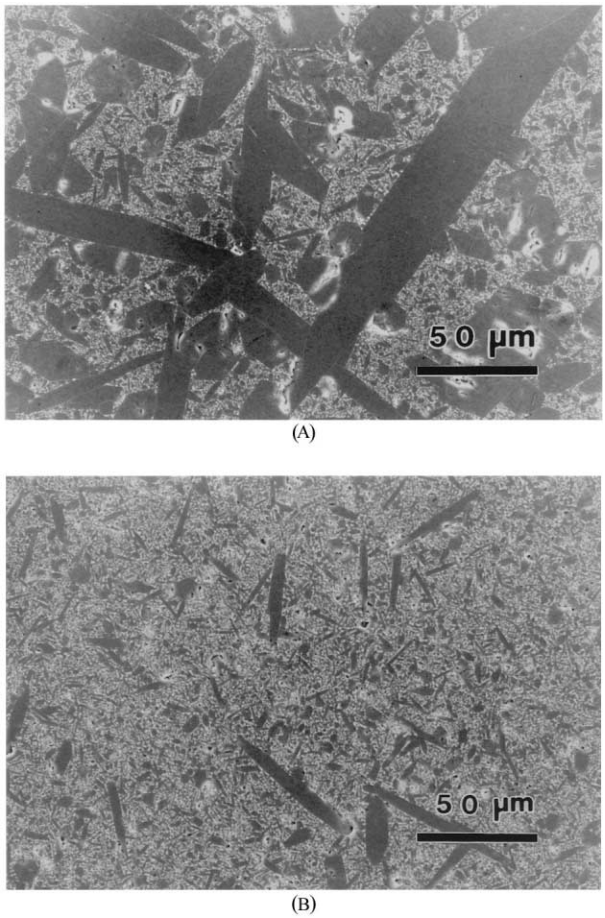

Fig. 1. Microstructure of investigated materials: (A) 0.5 mol% Nd_2O_3–0.5 mol% Y_2O_3-doped silicon nitride (SN1); (B) 2.0 mol% Nd_2O_3–2.0 mol% Y_2O_3-doped silicon nitride (SN4).

expressed as percent bending was adjusted to be lower than 5% at a stress of 60 MPa at room temperature. The percent bending (PB) is defined by [25]

$$\mathrm{PB} = \frac{\varepsilon_b}{\varepsilon_0} 100 \tag{1}$$

where

$$\varepsilon_b = \left[\left(\frac{\varepsilon_1 - \varepsilon_3}{2} \right)^2 + \left(\frac{\varepsilon_2 - \varepsilon_4}{2} \right)^2 \right]^{1/2}$$

$$\varepsilon_0 = \frac{\varepsilon_1 + \varepsilon_2 + \varepsilon_3 + \varepsilon_4}{4}$$

Specimens were heated under a pre-load of 98 N with a heating rate of 15°C/min. After reaching the test temperature, the temperature was maintained for about 15 min to ensure a uniform temperature gradient. The test load was then applied and the creep test started. Details of the experimental technique are described elsewhere.[20–24]

The microstructure after creep was examined with a transmission electron microscope (EM-002B, Topcon

Co. Ltd., Tokyo, Japan) at an accelerated voltage of 200 kV. Samples were cut from the crept specimens to be observed in the plane parallel to the tensile axis.

3. Results and discussion

Table 1 summarizes the creep test results of both silicon nitride materials. All the creep tests were performed at 1300°C and the stress was varied between 137 and 220 MPa. Creep deformation was observed in SN4 but not in SN1. It should be noted that the SN4 specimens were oxidized during the tests. The original colour was dark grey but after creep the colour of both the specimen surface and fracture surface was light grey. On the other hand, SN1 did not exhibit any colour change after creep due to its excellent oxidation resistance [6].

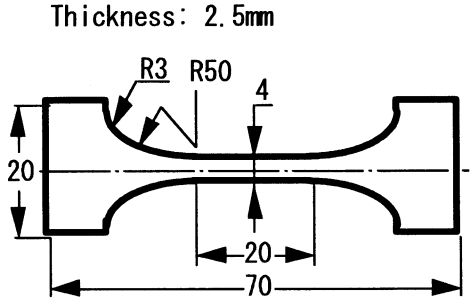

Fig. 2. Flat dog-bone specimen used for tensile creep tests.

Fig. 3 shows tensile creep curves of SN4 at 1300°C. It is clear that an increase in the stress leads to a higher creep rate and decrease in rupture time. In the creep curves for stresses of 137 and 150 MPa, a rapid increase in strain is seen in the initial stages, followed by a leveling out in the creep rate at longer times. In the cases of 180 and 200 MPa, however, the creep strain increased monotonically and it was difficult to identify the transient and steady state creep stages. The creep strains at fracture were in the range of 0.005 to 0.017 and the failure strain was greatest at a stress of 150 MPa. The lowest failure strain of 0.005 and the longest fracture time of 76.2 h was occurred for a stress level of 137 MPa.

Fig. 4 shows the stress dependence of SN4 on the creep rate at 1300°C. It is clear that the higher applied stress leads to a greater creep rate. The creep rate of the

Table 1
Summary of creep data

Specimen	Creep condition			Creep test results	
	Temperature (°C)	Test load (N)	Stress (MPa)	Time-to-rupture (h)	Minimum stress rate (s^{-1})
SN1-1	1300	2317.7	220.2	0.333 (20 min)	–
SN1-2	1300	2033.5	200.0	1	–
SN1-3	1300	1994.3	189.9	0.0167 (1 min)	–
SN1-4	1300	1832.6	179.9	0.25 (15 min)	–
SN1-5	1300	1528.8	149.9	20	–
SN1-6	1300	1411.2	137.0	11	–
SN4-1	1300	1499.4	150.2	29.5	1.15×10^{-7}
SN4-2	1300	1450.4	137.0	76.2	1.36×10^{-8}
SN4-3	1300	1817.9	179.8	9.5	3.97×10^{-7}
SN4-4	1300	1994.3	199.8	2.75	1.11×10^{-6}

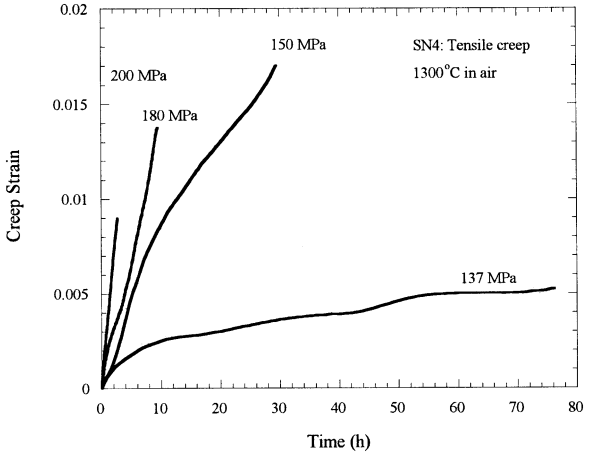

Fig. 3. Tensile creep curves of SN4 obtained at the indicated stresses at 1300°C.

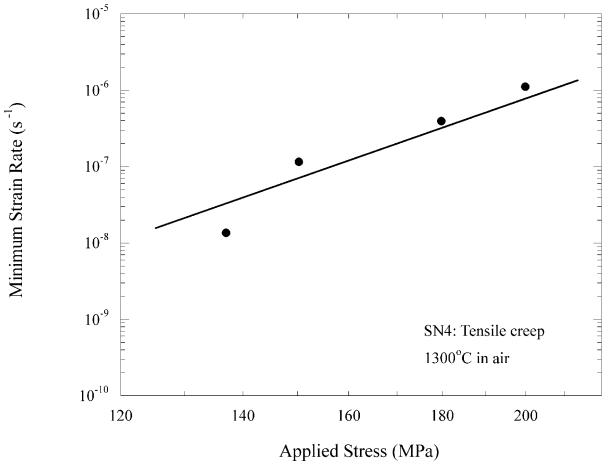

Fig. 4. Stress dependence of the minimum creep rate of SN4 at 1300°C. The stress exponent was calculated to be $n = 10.7$.

steady state stage, $\dot{\varepsilon}_{min}$, which is determined from the slope of the latter part of the creep curve, may be expressed by Norton's law as a power function of stress σ:

$$\dot{\varepsilon}_{min} = D\sigma^n \quad (2)$$

where n is the stress exponent. The value of n for SN4 at 1300°C was calculated to be 10.7. However, it should be noted that the true creep rate in the steady state region is somewhat lower because the creep rate gradually decreases with time and the minimum creep rate appears in the final part of the creep curve. In the present study, application of Norton's law may therefore be unsuitable in the strictest sense because in some cases the failure occurs at a stage where the strain rate gradually decreases with time. The apparent stress exponent can be determined from constant time and strain plots; for constant time plots, the stress exponent calculated from the minimum strain rate is at the lower end of the range, while in constant strain plots, higher n-values are obtained at small creep strains.[26] The values of the stress exponent obtained in the present study are, however, much greater than the predicted value from traditional creep mechanisms such as diffusion, viscous flow and solution-precipitation, and it is consistent with the value reported for tensile creep of silicon nitrides in which the cavitation mechanism governs.[7–14,17–19,21,24] Although the stress exponent n in Eq. (2) is sometimes greater at higher stress due to the contribution of intensive cavitation to the creep deformation,[27,28] such behavior was not observed in the stress versus strain rate plots in the present study. It should be noted that the high stress exponent value of $n = 10.7$ is consistent with the prediction from the cavitational creep model by Luecke and Wiederhorn.[29] They calculated a cavitational creep rate from the apparent viscosity of a fluid packed with particles, and revealed the exponential dependence of the creep rate on applied stress. Therefore, a detailed description of cavitational creep behavior may require a modified model rather than Norton's law.

The relationship between time-to-failure t_f and the minimum strain rate $\dot{\varepsilon}_{min}$ may be described by the Monkman–Grant relation[30]

$$t_f = C\dot{\varepsilon}_{min}^{-m} \quad (3)$$

where m is the Monkman–Grant constant, usually close to one. Combining Eqs. (2) and (3), the time-to-failure can be expressed as[16]

$$t_f = B\sigma^{-N} \quad (4)$$

where $N = nm$ and B is a constant. This equation can also be derived from Larson–Miller analysis with a constant temperature.[31,32] Moreover, the same expression can be derived from the equation of subcritical crack growth velocity, which describes the subcritical crack growth velocity v as a function of stress intensity K_I

$$v = AK_I^N \quad (5)$$

It should be noted that in the case of delayed failure resulting from subcritical crack growth the time-to-failure depends on the size of pre-existing flaws while in the case of creep rupture the flaw responsible for the failure is produced during creep.[16] Fig. 5 shows the time-to-failures of SN4 at 1300°C under a tensile stress ranging from 137 to 200 MPa. It is clear that a decrease in the stress results in an increase in the rupture time. The value of N in Eq. (2) is calculated to be 8.4 for SN4 at 1300°C. Since $n = 10.7$, the Monkman–Grant parameter of m is estimated to be 0.79. This estimate seems to be a little smaller because the plots of the minimum strain rate against time-to-failure lead to a value of $m = 1.28$ (Fig. 6). This may be attributed to the overestimated stress exponent value due to an insufficient number of

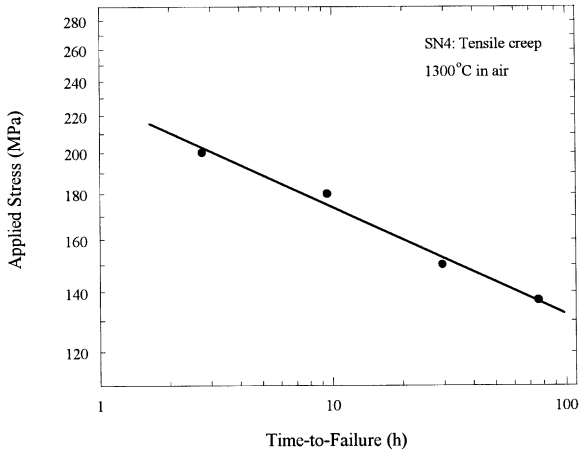

Fig. 5. Time-to-failure of 2.0 mol% Nd_2O_3–2.0 mol% Y_2O_3-doped silicon nitride (SN4) at 1300°C under a tensile stress ranging from 137 to 200 MPa. The stress–rupture parameter was calculated to be $N = 8.4$.

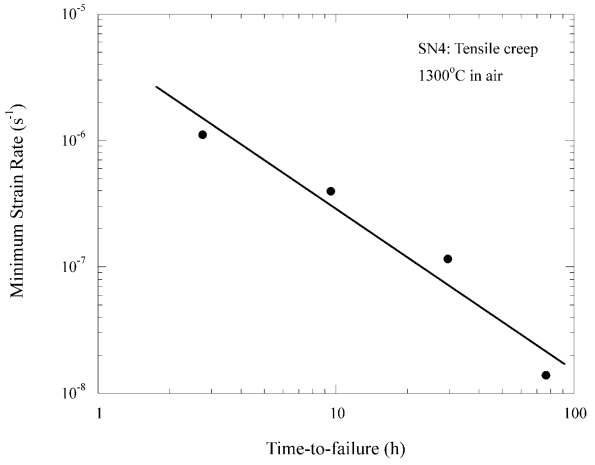

Fig. 6. Plots of the minimum strain rate against time-to-failure of SN4 at 1300°C. The Monkman–Grant parameter was determined to be $m = 1.28$.

data points and the difficulty in identifying the transient and steady state creep stages. The Monkman–Grant parameter is in general more than one and close to unity, assuming that the failure strain gradually decreases with an increase in the creep rate.[33]

Six tensile specimens of SN1 were tested at 1300°C. Times-to-failure for the tests at 180 MPa or more were shorter than 1 h and the longest fracture time was 20 h at a stress of 150 MPa. During the tests, no creep strains were detected. The small creep strains are likely to be due to the small amount of additives. Lange et al. investigated the compression creep of hot pressed silicon nitrides with MgO additions of 2 and 5%, and reported that the creep rate is several times greater for 5% MgO than 2%.[9] However, the difference in creep rates seems to be much greater in the present study, in spite of the fact that there are no available creep rate data for SN1. Fig. 7 shows time-to-failure plotted against the applied stress. Despite the large scatter in data, it can be seen that the time-to-failure increases with a decrease in the applied stress. The N value of SN1 at 1300°C was 20.7. This N value could have some meaning as a subcritical crack growth parameter since no creep strains were detected. Table 2 summarizes the stress exponents and the stress-rupture parameters for both SN1 and SN4 at 1300°C.

Table 2
Stress exponents and stress rupture parameters for silicon nitrides at 1300°C

Materials	Testing temperature (°C)	Stress exponent (n)	Stress–rupture parameter (n)
Silicon nitride: SN1	1300	–	20.7
Silicon nitride: SN4	1300	10.7	8.4

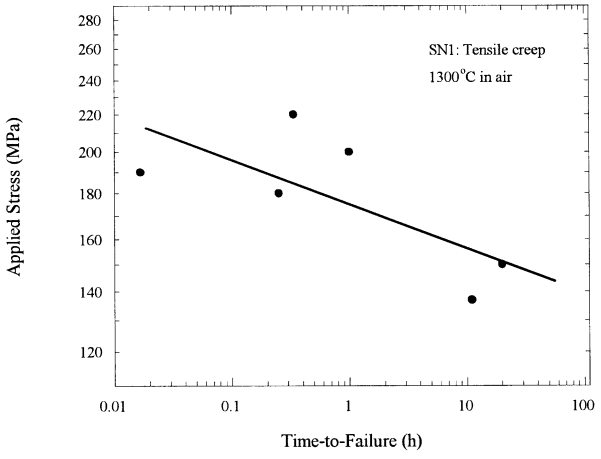

Fig. 7. Time-to-failure of SN1 (0.5 mol% Nd_2O_3–0.5 mol% Y_2O_3-doped silicon nitride) at 1300°C under a tensile stress ranging from 137 to 220 MPa. The stress–rupture parameter was determined to be $N = 20.7$.

Fig. 8 shows a transmission electron micrograph of 2.0 mol% Nd_2O_3–2.0 mol% Y_2O_3-doped silicon nitride crept at 1300°C for 29.5 h under a stress of 150 MPa. This shows that the secondary phase has crystallized and a considerable amount of cavities are seen in the triple junctions. The high stress exponent of SN4 is consistent with this observation of intensive cavitation. Moreover, small precipitates are seen in the silicon nitride grains (e.g. the left most grain in Fig. 8B). Fig. 9 shows the energy-dispersive X-ray spectroscopy (EDS) analysis of a secondary phase found in this sample (marked a in Fig. 9A). The diffraction pattern of the secondary phase shown in Fig. 9A reveals the presence of a crystalline phase. The EDS analysis of the secondary phase shown in Fig. 9B indicates that the elements

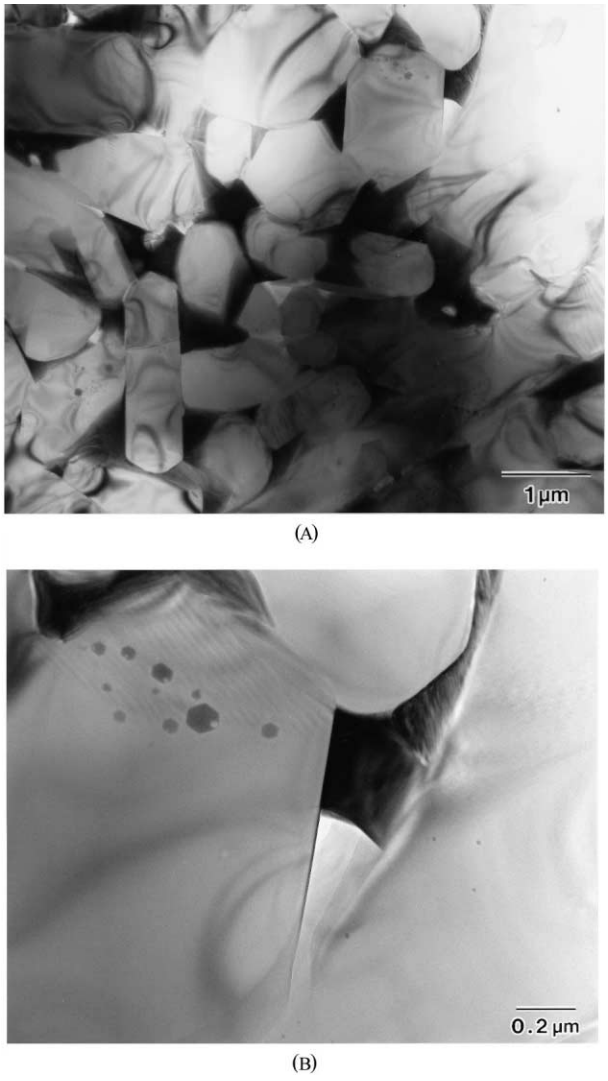

Fig. 8. Transmission electron micrograph of 2.0 mol% Nd_2O_3–2.0 mol% Y_2O_3-doped silicon nitride crept at 1300°C for 29.5 h under a stress of 150 MPa. (A) Low magnification micrograph indicating the crystallized secondary phase and cavities developed in the triple junctions. (B) Close up of triple junction and surrounding silicon nitride grains. Precipitates are seen in the left most grain of silicon nitride.

Nd, Y and Si are present in the secondary phase. The presence of Mg and Ca is likely due to the migration of contaminants during processing. The transmission electron micrograph in Fig. 10A shows precipitates in a silicon nitride grain and Fig. 10B shows the EDS analysis of the precipitate marked b in Fig. 10A. EDS analysis indicates that Nd, Y and Si are present in the precipitate and the chemical composition is similar to the secondary phase found in Fig 9. Again, the Mg and Ca found in the precipitate are probably due to contamination during processing.

It has been reported that an amorphous phase of approximately 1 μm is present at the triple junction of 5.0 mol% Nd_2O_3–5.0 mol% Y_2O_3-doped silicon nitride.[34,35] Furthermore, EDS analysis revealed that rare earth elements are present in the grain boundary amorphous phase between two silicon nitride grains, and that the triple junction is amorphous and heterogeneous in composition, with the concentration of rare earth elements being higher in the central zone.[34] In the present study, however, the triple junction seems to have uniform chemical composition because it is a fully crystalline solid.

Fig. 11 shows a transmission electron micrograph of 0.5 mol% Nd_2O_3–0.5 mol% Y_2O_3-doped silicon nitride (SN1) crept at 1300°C for 20 h under a stress of 150 MPa. The low magnification micrograph shown in Fig. 11A indicates that the secondary phases are crystallized and that a small number of cavities are generated in some of the triple junctions, even for small creep

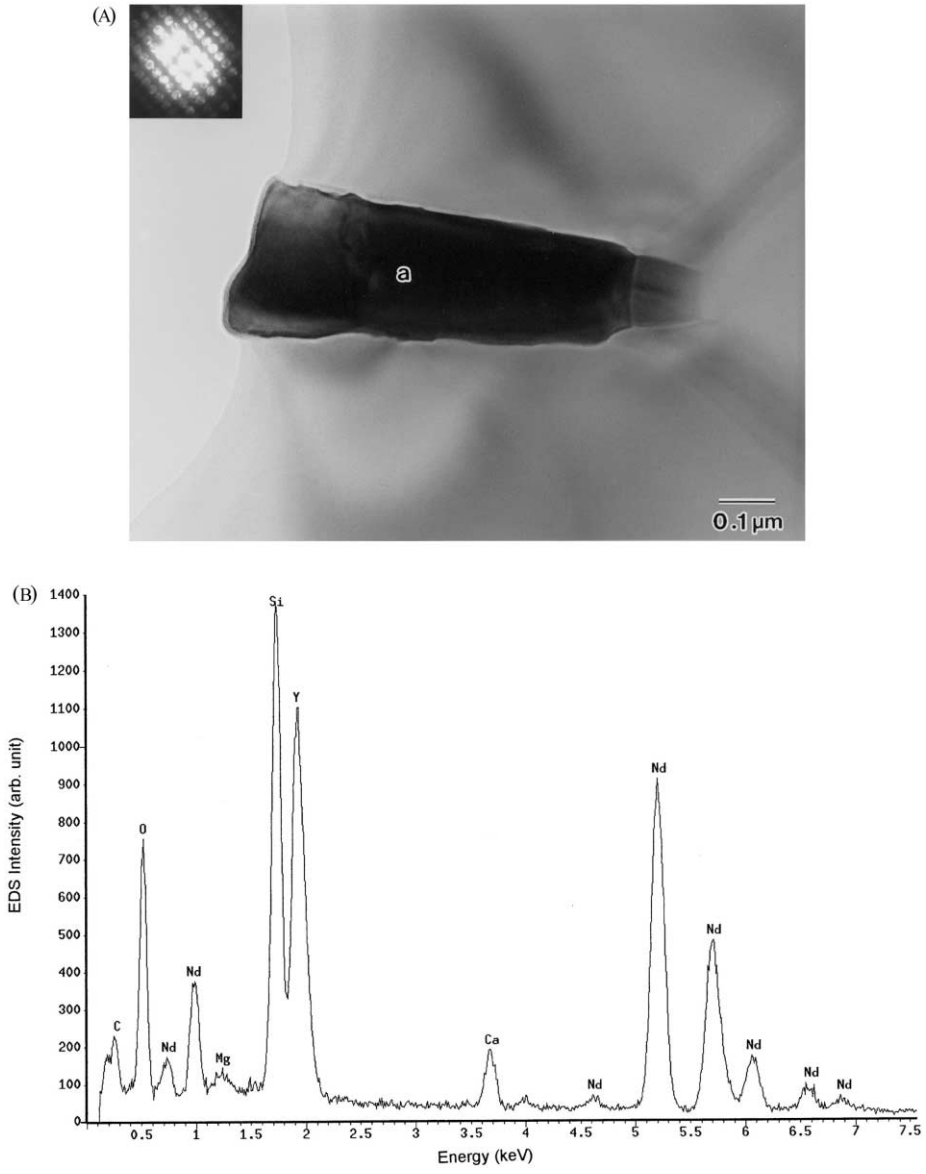

Fig. 9. EDS analysis of a secondary phase (marked a) found in the crept specimen of 2.0 mol% Nd_2O_3–2.0 mol% Y_2O_3-doped silicon nitride at 1300°C for 29.5 h under a stress of 150 MPa. (A) Transmission electron micrograph with diffraction pattern of the secondary phase, indicating a crystalline phase. (B) The EDS analysis of the secondary phase indicating that the elements Nd, Y and Si are present.

strain. Fig. 11B shows a transmission electron micrograph with higher magnification. The diffraction pattern of the secondary phase (marked c) shows clear spots, indicating a crystalline phase. In addition, small precipitates are seen in the silicon nitride grains (e.g. the right grain of Fig. 11B). These precipitates are similar to those found in Fig. 10A although they are somewhat larger in size.

It has been reported that a glassy boundary phase of approximately 1 nm with high SiO_2 concentration and low Y and Nd concentrations is present between two silicon nitride grains in SN1 before creep, and that there is a glassy phase in the triple junctions, in which the concentration of Nd is higher in the center than near the edge.[34] In the present study, a crystalline phase was found at triple junctions. This suggests that the transition from the amorphous to crystalline phase occurs during heat treatment in the creep test.

From the comparison between microstructures of these silicon nitrides (see Figs. 8A and 11A), it is clear that the amount of grain boundary phase is much smaller in SN1 than SN4, leading to the lower creep rate of SN1. Moreover, the elongated large silicon nitride grains are greater in SN1 than in SN4 (see Fig. 1). Since the creep rate due to the solution-precipitation mechanism is smaller in materials having larger grains,[36] the large elongated grains can reduce the creep rate. In addition, such large elongated grains may easily interlock each

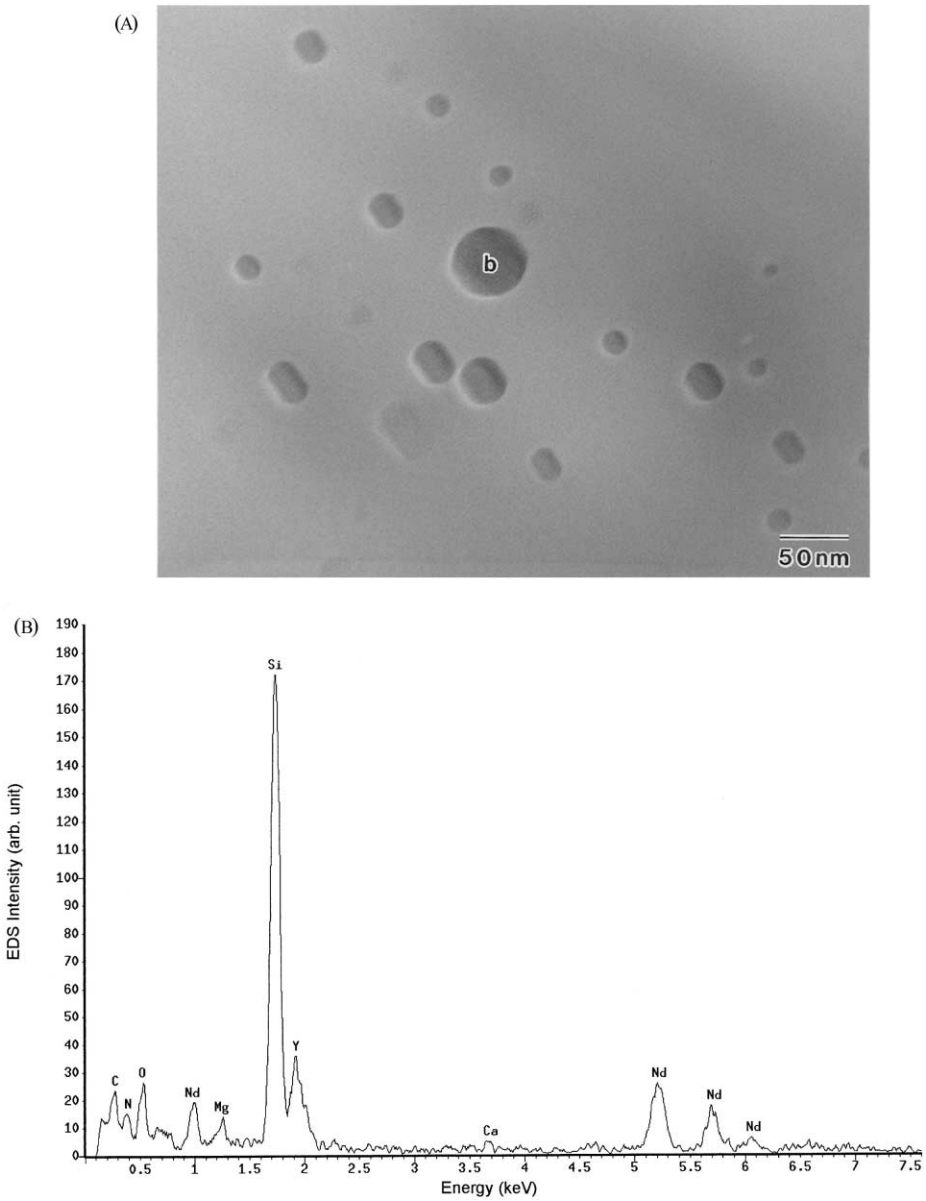

Fig. 10. EDS analysis of the precipitate (marked b) in a silicon nitride grain found in the crept specimen of 2.0 mol% Nd_2O_3–2.0 mol% Y_2O_3-doped silicon nitride at 1300°C for 29.5 h under a stress of 150 MPa. (A) Transmission electron micrograph showing the precipitate in the silicon nitride grain. (B) EDS analysis of the precipitate phase, indicating that the elements Nd, Y and Si are present.

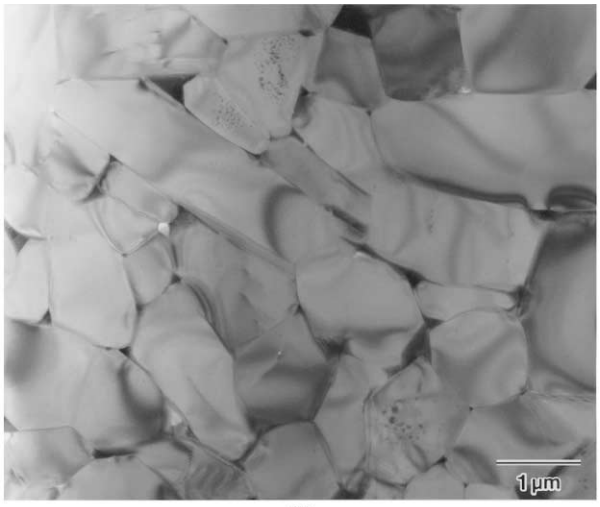

(A)

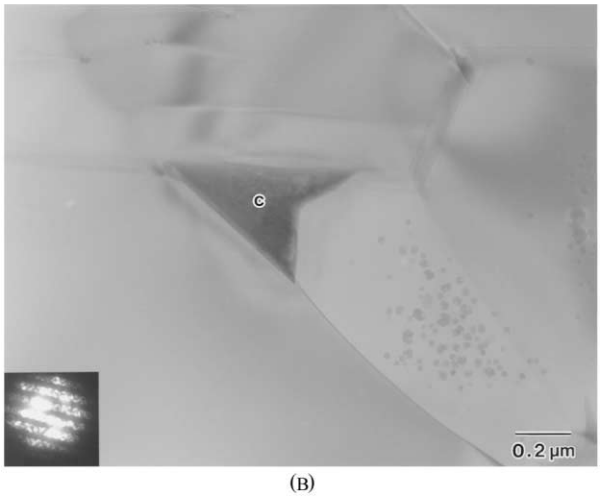

(B)

Fig. 11. Transmission electron micrographs of 0.5 mol% Nd_2O_3–0.5 mol% Y_2O_3-doped silicon nitride (SN1) crept at 1300°C for 20 h under a stress of 150 MPa. (A) Low magnification micrograph, indicating that cavities are present in some triple junctions. (B) Close up of a triple junction (marked c) with diffraction pattern, indicating that the secondary phase is crystalline. Small precipitates are seen in the right most grain of silicon nitride.

other to impede further deformation. However, this mechanism allows initial deformation until the grains contact each other, and interlocking occurs easily in materials having a low amount of liquid phase.[37,38] Therefore, the most plausible reason for the excellent creep resistance in SN1 seems to be the smaller amount of grain boundary phase rather than grain morphology.

4. Summary

Tensile creep tests were performed on two silicon nitride materials containing different amounts of sintering aids. 2.0 mol% Nd_2O_3–2.0 mol% Y_2O_3-doped silicon nitride (SN4) exhibited significant deformation and the stress exponent was $n = 10.7$, while 0.5 mol% Nd_2O_3–0.5 mol% Y_2O_3-doped silicon nitride (SN1) exhibited no creep deformation at 1300°C. The stress-rupture parameter, N, was determined to be 8.4 for SN4 and 20.7 for SN1. The high stress exponent found in SN4 suggests that cavitation creep is dominant in this case. This was consistent with creep damage observations from transmission electron microscopy, which revealed numerous cavities present in the triple junction. In addition, the similarity in the values between the stress exponent and stress-rupture behavior suggests that the dominant mechanism in SN4 at 1300°C is not subcritical crack growth but creep rupture. In contrast, the stress-rupture parameter obtained for SN1 is thought to correspond to the subcritical crack parameter since SN1 exhibited no creep deformation.

Acknowledgements

We would like to thank Mr. T. Suzuki for helpful discussions and assisting with TEM work, and Mr. Y. Yamamoto for preparing specimens. The work was conducted under the High Temperature Materials 21 project, promoted by the Science and Technology Agency of Japan.

References

1. Hirosaki, N., Okada, A. and Matoba, K., Sintering of Si_3N_4 with the addition of rare-earth oxides. *J. Am. Ceram. Soc.*, 1988, **71**, C144–C147.
2. Hirosaki, N., Okada, A. and Akimune, Y., Gas pressure sintering of silicon nitride containing small amounts of oxide additives. *J. Mater. Sci. Lett.*, 1990, **9**, 1322–1323.
3. Hirosaki, N. and Okada, A., Dense silicon nitride containing low amounts of Y_2O_3 and Nd_2O_3. *Nippon Seramikkusu Kyokai Gakujutsu Ronbunshi*, 1989, **97**, 673–675.
4. Hirosaki, N. and Okada, A., Effect of additive-oxide amount on sintering of Si_3N_4 with Y_2O_3 and Nd_2O_3. *J. Mater. Sci.*, 1992, **27**, 3743–3748.
5. Hirosaki, N. and Okada, A., Change in oxygen content of Y_2O_3–Nd_2O_3-doped silicon nitride during firing. *J. Am. Ceram. Soc.*, 1989, **72**, 2359–2360.
6. Hirosaki, N., Akimune, Y., Ogasawara, T. and Okada, A., Effect of additive amounts on oxidation of Y_2O_3–Nd_2O_3-doped silicon nitride. *J. Mater. Sci. Lett.*, 1991, **10**, 753–755.
7. Kossowsky, R., Miller, D. G. and Diaz, E. S., Tensile and creep strengths of hot-pressed Si_3N_4. *J. Mater. Sci.*, 1975, **10**, 983–997.
8. Seltzer, M. S., High temperature creep of silicon-base compounds. *Am. Ceram. Soc. Bull.*, 1977, **56**, 418–423.
9. Lange, F. F., Diaz, E. S. and Anderson, C. A., Tensile creep testing of improved Si_3N_4. *Am. Ceram. Soc. Bull.*, 1979, **58**, 845–848.
10. Aron, R. M. and Tien, J. K., Creep and strain recovery in hot-pressed silicon nitride. *J. Mater. Sci.*, 1980, **15**, 2046–2058.
11. Ferber, M. K. and Jenkins, M. J., Evaluation of the strength and creep-fatigue behavior of hot isostatically pressed silicon nitride. *J. Am. Ceram. Soc.*, 1992, **75**, 2453–2462.
12. Ding, J.-L., Liu, K. C., More, K. L. and Brinkman, C. R., Creep and creep rupture of an advanced silicon nitride ceramic. *J. Am. Ceram. Soc.*, 1994, **77**, 867–874.

13. Ferber, M. K., Jenkins, M. J., Nolan, T. A. and Yeckley, R. L., Comparison of creep and creep rupture performance of two HIPed silicon nitride ceramics. *J. Am. Ceram. Soc.*, 1994, **77**, 657–665.
14. Gasgaska, C. J., Tensile creep in an in situ reinforced silicon nitride. *J. Am. Ceram. Soc.*, 1994, **77**, 2408–2418.
15. Wiederhorn, S. M., Hockey, B. J., Cranmer, D. C. and Yeckley, R., Transient creep behaviour of hot isostatically pressed silicon nitride. *J. Mater. Sci.*, 1993, **28**, 445–453.
16. Wiederhorn, S. M., French, J. D., and Luecke, W. E. B., High temperature reliability of silicon nitride. In *5th International Symposium on Ceramic Materials and Components for Engines*, ed D.S. Yan, X. R. Fu and S.X. Shi. World Scientific Publishing Co, Singapore, 1995, pp. 145–155.
17. Luecke, W. E., Wiederhorn, S. M., Hockey, B. J., Krause, R. F. and Long, G. G., Cavitation contributes substantially to tensile creep in silicon nitride. *J. Am. Ceram. Soc.*, 1995, **78**, 2085–2096.
18. Krause, R. F., Luecke, W. E., French, J. D., Hockey, B. J. and Wiederhorn, S. M., Tensile creep and rupture of silicon nitride. *J. Am. Ceram. Soc.*, 1999, **82**, 1233–1241.
19. Wereszczak, A. W., Ferber, M. K., Kirkland, T. P., Barnes, A. S., Frome, E. L. and Menon, M. N., Asymmetric tensile and compressive creep deformation of hot-isostatically-pressed Y_2O_3-doped Si_3N_4. *J. Eur. Ceram. Soc.*, 1998, **19**, 227–237.
20. Lofaj, F., Usami, H., Okada, A. and Kawamoto, H., Long-term creep damage development in a self-reinforced silicon nitride. In *Engineering Ceramics '96: Higher Reliability Through Processing*, ed. C. N. Babini, M. Haviar and P. Sajgalih. Kluwer Academic Publishers, Dordrecht, The Netherlands, 1997, pp. 337–352.
21. Lofaj, F., Cao, J.-W., Okada, A. and Kawamoto, H., Comparison of creep behavior and creep damage mechanisms in the high-performance silicon nitrides. In *6th International Symposium on Ceramic Materials and Components for Engines*, ed. K. Niihara, S. Komeya, K. Komeya, S. Hirano and K. Morinaga. Technoplaza, Tokyo, Japan, 1997, pp. 713–718.
22. Lofaj, F., Okada, A. and Kawamoto, H., Creep damage in an advanced self-reinforced silicon nitride: part I, cavitation in the amorphous boundary phase. *J. Am. Ceram. Soc.*, 1999, **84**, 1009–1019.
23. Okada, A. and Lofaj, F., Elastic degradation of an advanced silicon nitride during tensile creep. *J. Eur. Ceram. Soc.*, 2000, **20**, 1521–1525.
24. Okada, A., Cao, J.-W., and Lofaj, F., Creep lifetime prediction for advanced silicon nitrides in 300 kW ceramic gas turbine. In *Proceedings of the International Symposium on Environment Conscious Materials — Ecomaterials*, ed. H. Mostaghaci. The Canadian Institute of Mining, Metallurgy and Petroleumo, Ottawa, Canada, 2000, pp. 741–755.
25. Standard test method for elevated temperature tensile creep strain, creep strain rate, and creep time-to-failure for advanced monolithic ceramics. ASTM Designation: C 1291-95, The American Society for Testing and Materials, Philadelphia, PA, USA, 1995.
26. Grathwohl, G., Regimes of creep and slow crack growth in high-temperature rupture of hot-pressed silicon nitride. In *Material Science Research Vol. 18, Deformation of Ceramic Materials II*, ed. R. E. Tressler and R. C. Bradt. Plenum Press, New York, 1984, pp. 573–586.
27. Wiederhorn, S. M., Roberts, D. E., Chuang, T.-J. and Chuck, L., Damage-enhanced creep in a siliconized silicon carbide: phenomenology. *J. Am. Ceram. Soc.*, 1988, **71**, 602–608.
28. Carrol, D. F. and Tressler, R. E., Effect of creep damage on the tensile creep behavior of a siliconized silicon carbide. *J. Am. Ceram. Soc.*, 1989, **72**, 49–53.
29. Luecke, W. E. and Wiederhorn, S. M., A new model for tensile creep of silicon nitride. *J. Am. Ceram. Soc.*, 1999, **82**, 2769–2778.
30. Monkman, F. C. and Grant, N. J., An empirical relationship between rupture life and minimum strain rate in creep-rupture tests. *Proc. Am. Soc. Test. Mater.*, 1956, **56**, 593–630.
31. Larson, F. R. and Miller, J., A time-temperature relationship for rupture and creep stress. *Trans. ASME*, 1952, **74**, 765–775.
32. Deng, S. and Warren, R., Creep properties of single crystal oxides evaluated by a Larson–Miller procedure. *J. Eur. Ceram. Soc.*, 1995, **15**, 513–520.
33. Hockey, B. J., Wiederhorn, S. M., Liu, W., Baldoni, J. G. and Buljan, S.-T., Tensile creep of whisker-reinforced silicon nitride. *J. Mater. Sci.*, 1991, **26**, 3931–3939.
34. Bando, Y., Mitomo, M. and Kurashima, K., An inhomogeneous grain boundary composition in silicon nitride ceramics as revealed by 300 kW field emission analytical electron microscopy. *J. Materials Synthesis and Processing*, 1998, **6**, 359–365.
35. Hirosaki, N., Inoue Y., Akimune, Y., TEM analysis of grain boundary in Y_2O_3–Nd_2O_3-doped silicon nitride. *J. Ceram. Soc. Jpn.*, 1992, **100**, 720–724 (in Japanese).
36. Raj, R. and Chyung, C. K., Solution-precipitation creep in glass ceramics. *Acta Metall.*, 1981, **29**, 159–166.
37. Muto, H. and Sakai, M., Grain-boundary sliding and grain interlocking in the creep deformation of two-phase ceramics. *J. Am. Ceram. Soc.*, 1998, **81**, 1611–1621.
38. Sakai, M., Muto, H. and Haga, M., Stress relaxation of polycrystalline ceramics with grain-boundary sliding and grain interlocking. *J. Am. Ceram. Soc.*, 1999, **82**, 169–177.